

Article

Field Campaign on Pressure on the Crown Wall at the Outer Port of Punta Langosteira Breakwater

José Sande ^{1,*}, Maria Graça Neves ², José-Santos López-Gutiérrez ^{3,*}, M. Dolores Esteban ³, Andrés Figuero ^{1,*} and Vicente Negro ³

¹ Water and Environmental Engineering Group (GEAMA), Universidad de A Coruña, 15071 A Coruña, Spain

² Nova School of Science and Technology (FCT NOVA), Universidade NOVA de Lisboa, Campus de Caparica, 2829-516 Caparica, Portugal

³ Environment, Coast and Ocean Research Laboratory (ECOREL-UPM), Universidad Politécnica de Madrid, 28040 Madrid, Spain

* Correspondence: jose.sande@udc.es (J.S.); jos santos.lopez@upm.es (J.-S.L.-G.); andres.figuero@udc.es (A.F.)

Abstract: Punta Langosteira port, located in A Coruña (Spain), was monitored during the winters of 2017 and 2018, measuring wave pressure in the crown wall structure. Furthermore, the metocean variables were measured on a buoy located very close to the breakwater. This paper presents the real pressures measured at the crown wall of the breakwater during different storm events. These values are compared with the results of the application of state-of-the-art equations for the calculation of pressures on crown walls. The results obtained show the behaviour of the pressures with a crown wall fully protected by the armour, as is the case of Langosteira breakwater. Finally, several conclusions are made on the methodology for measuring the pressures using physical models and the relevance of the armour roughness.

Keywords: crown wall; rubble mound breakwater; field campaign; pressure

Citation: Sande, J.; Neves, M.G.; López-Gutiérrez, J.-S.; Esteban, M.D.; Figuero, A.; Negro, V. Field Campaign on Pressure on the Crown Wall at the Outer Port of Punta Langosteira Breakwater.

J. Mar. Sci. Eng. **2022**, *10*, 1377. <https://doi.org/10.3390/jmse10101377>

Academic Editor: Theofanis Karambas

Received: 24 August 2022
Accepted: 22 September 2022
Published: 26 September 2022

Publisher's Note: MDPI stays neutral with regard to jurisdictional claims in published maps and institutional affiliations.



Copyright: © 2022 by the authors. Licensee MDPI, Basel, Switzerland. This article is an open access article distributed under the terms and conditions of the Creative Commons Attribution (CC BY) license (<https://creativecommons.org/licenses/by/4.0/>).

1. Introduction

Port breakwaters are key infrastructures for maritime transport as their presence shelters ships from waves so that ships can safely carry out their operations safely in the port [1,2]. One of the most common types of breakwaters are rubble mound ones, which are an accumulation of material in an orderly way consisting of different components: armour, filters, core, berm, and crown wall. Breakwaters with crown walls require less material, and thus less occupation of the seabed and consequently a lower impact, to achieve the same overtopping rate as those without crown walls [3–5]. In fact, nowadays, it is most common to find and design seawalls with crown walls.

There are different types of crown walls, whether we consider the type of material they are made of or their shape, although they all have the same function. Crown wall design methods are not as widespread as those for other parts of rubble mound breakwaters such as the armour, filter, and so on. As the crown wall is a critical part of the breakwater, a reliable design equation is critical [6,7].

Calculating the forces on the crown walls is a complex task that is critical for an adequate design of the breakwater. There have been several failures in breakwater crown walls, so it is evident that their design must be based on experience. Moreover, the existing equations to design crown walls are based on physical models and the limitations of their use are based on the conditions in the tests used to develop them at the laboratory. So, the first step in the design of crown walls is to select the equation or equations to be used given the geometrical condition of the specific breakwater to be designed and the wave conditions of the zone.

There are several existing equations for crown wall design including Iribarren and Nogales (1964) [8], Jensen (1984) [9] and Bradbury et al. (1998) [10], Günback and Gökçe (1984) [11], Martin et al. (1999) [12], Berenguer and Baonza (2006) [3,5], Pedersen (1996) [13,14], and Nørgaard et al. (2013) [15]. Most of these equations have been obtained as laboratory test results, each of them covering boundary conditions outside of which the equations are not reliable [16–20].

Nowadays, these formulas are starting to be applied for a great variety of wave conditions and sea levels [21], some of them out of the limit of the application of equations, which is most important considering the phenomenon of climate change [22–26].

Although the ideal is to have field trials at a 1:1 scale to verify formulas, this is not always feasible given the cost of implementation, the time it takes to analyse them to contemplate different storms, and so on. In addition, instrumentation in nature in such an aggressive environment is not always easy to install, maintain, and operate.

This leads to uncertainty when it comes to obtaining the actions to calculate the stability of the crown wall. Validating the most suitable equations with a 1:1 scale test is a must that would help to take an important step in the state-of-the-art of crown wall design. Therefore, the motivation of this research and this article is to analyse with real instrumentation results the reliability of the equation results, as well as to identify the lessons learned from laboratory tests that lead to most of this type of equation, as well as from field measurements at a 1:1 scale crown wall. The real case presented here is the Port of Langosteira, Spain, where one section of the breakwater was instrumented with eight pressure sensors, with five of them located on the front wall of the crown wall and the other three placed on top of the crown wall.

2. Methods

This manuscript aims to analyse field data obtained during eight storm events on the front face of one cross section of the crown wall at the Punta Langosteira Outer Port. Specifically, eight pressure sensors were deployed in one cross section of the main breakwater, five of which allow one to study the pressure on the crown wall front face, exposed to the waves, while the other three are to study the overtopping events on this cross section. In addition, the port has a directional wave buoy in the vicinity of the port, enabling to have simultaneous information of metocean variables.

The data presented here were obtained from the field campaign developed during the winter of 2017/2018. Eight storm events led to no null horizontal pressure registered on the eight pressure sensors. In these events, pressures in the mentioned cross section were recorded.

The methodology applied in this work has two main objectives. The first one is the analysis of the pressure data measured by the pressure sensors located in the front face of the crown wall. This information makes it possible to explain the water behaviour at the crown wall and the causes of the maximum pressure peaks. The second goal is to compare the measured pressure values with the ones resulting from the application of the different existing equations for the design of crown walls, enabling us to analyse their applicability in crown walls with similar characteristics.

Wave conditions and water levels, as well as cross-sectional characteristics, enable the estimation of maximum horizontal pressure using formulas available in the literature. Not all formulas presented in the literature estimate pressures and are valid for crown walls fully protected by the armour layer. Here, the formulas used to estimate the pressure of the front wall are as follows: (1) Günback and Gökçe (1984) [11]; (2) Martin et al. (1999) [12]; and (3) Nørgaard et al. (2013) [15]. Formulas that directly calculate forces, such as Berenguer and Baonza (2006) [3,5] or Jensen (1984) [9] and Bradbury et al. (1988) [10], were not considered.

The following chapters show the results obtained in the two methodological stages described before, as well as the conclusions obtained in the analysis of the breakwater crown wall fully protected by pieces of the protection armour.

3. Description of the Case Study

The cross section of the Punta Langosteira rubble mound breakwater monitored is described. The pressures measured in the front face of the crown wall during the winter of 2017/2018 storm events are presented and analysed here.

3.1. Rubble Mound Breakwater Description

The outer port of Punta Langosteira (Figure 1) is protected by a 3360 m main breakwater, developed in three alignments with a toe at a maximum depth of 45 m. In addition, the port is also protected by a secondary breakwater, the western breakwater, composed of Cubipod® (SATO, Madrid, Spain) [27].



Figure 1. Punta Langosteira Outer Port and the western breakwater. Location of the cross section monitored [28].

The main breakwater has a 2:1 slope, protected by a double layer of cubic blocks of 150 tons in the trunk. The crowning height of the crown wall is +25 m, and it has a zone of 20 m wide partially protected by a perimeter gallery. The upper berm of the armour layer is as high as the crest elevation of the crown wall. In other words, the crown wall is fully protected by the blocks of the armour layer. The crown wall crest level means that the overtopping occurs only for the larger wave heights.

Within the Cormoran project, the engineering firm Eptisa—Ingeniería, Instrumentación y Control (IIC) installed eight pressure sensors in one cross section of the main breakwater called Section PK 2 + 883. There, the structure is composed of a protective armour formed by two layers of cubic blocks of 150 ton placed randomly. Below this layer is a first filter formed by cubic blocks of 15 ton, which in turn rests on a 1-ton rock layer. Both the cross section and the sensors' location are shown in Figure 2. As can be seen in Figure 2, the underlayer consists of a 5-ton rock above the mean sea level and a 1-ton rock beneath it.

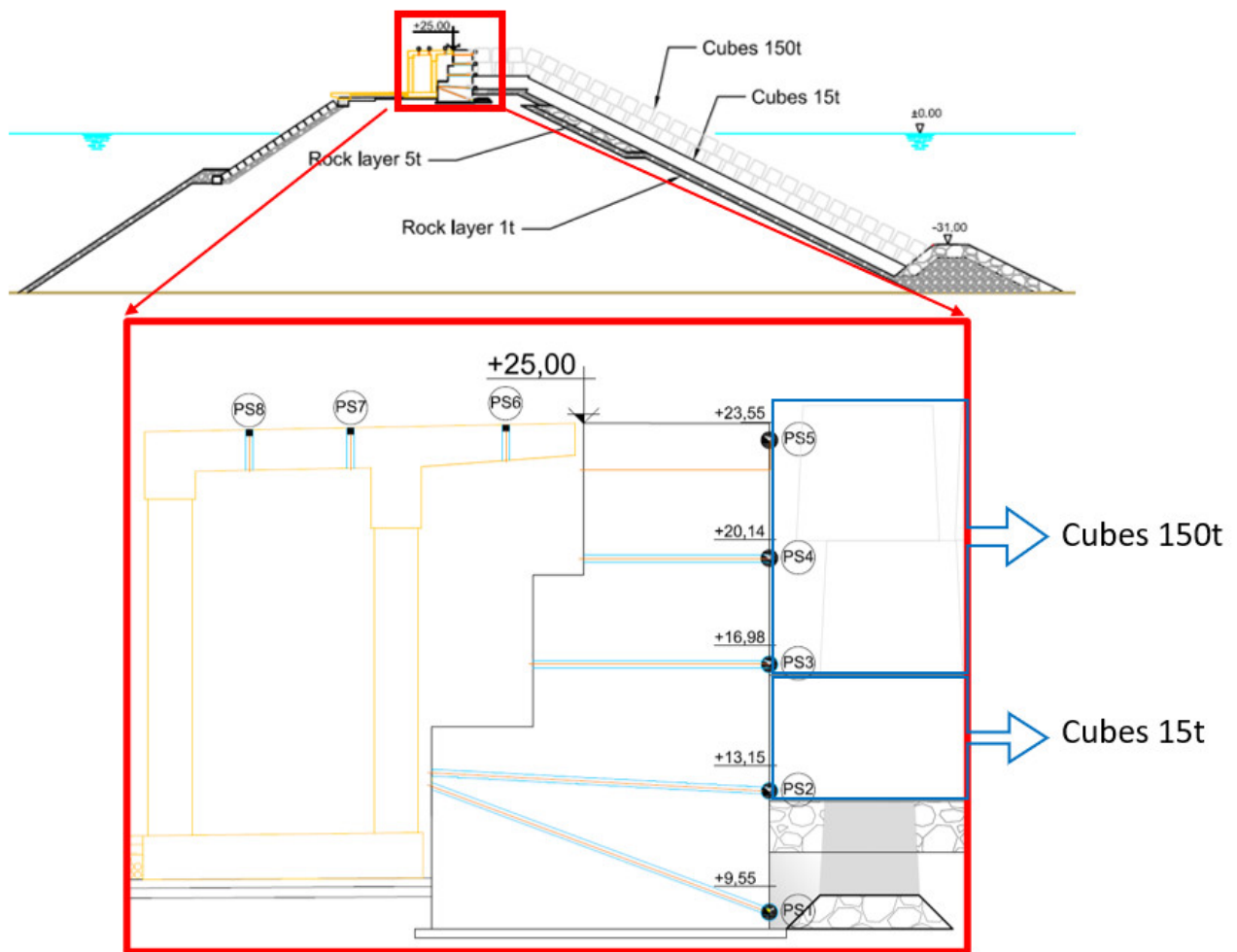


Figure 2. Schematic view of the cross section and the instrumentation.

Pressure sensors were regularly distributed along the front face of the crown wall, starting from the base (PS1) to the top of the crown wall (PS5). There is a cube placed just in front of pressure sensors PS1 and PS2. PS1 is in front of the rubble mound foundation of the cube. Pressure sensor 2 is in front of the first filter and pressure sensors PS3 to PS5 are in front of the main armour layer. All of them are more than 9.55 m above the chart datum (CD). PS6 to PS8 sensors are placed in the crown of the perimeter gallery and have helped to identify if the overtopping phenomenon occurs when the pressure was measured. These sensors give information about overtopping occurrence.

Figure 3 shows the main parameters of the monitored cross section, and Table 1 presents their values. The outer main armour layer has a 1:2 slope. The distance from the crown of the superstructure in relation to the sea level (R_c) and the distance from the superstructure foundation in relation to the sea level (F_c) depends on the water level considered.

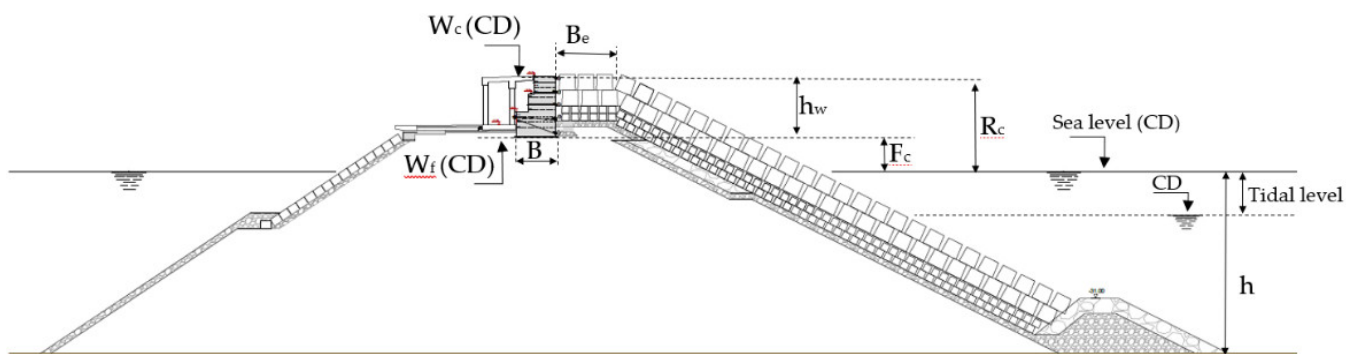


Figure 3. Main parameters of the cross section.

Table 1. Values of the main parameters of the cross section.

Parameter	Value
Be	24.05 m (CD)
h	45.8 m
hw	6.0 m
B	10.0 m
Wc	24.0 m (CD)
Wf	9.05 m

Finally, an important element is the crown wall configuration in the area where the sensors are located. Figure 4 shows an aerial view of the analysis area, where it can be seen how the sensors are placed just behind a block of the armour layer, which will be relevant when analysing the results and drawing conclusions.

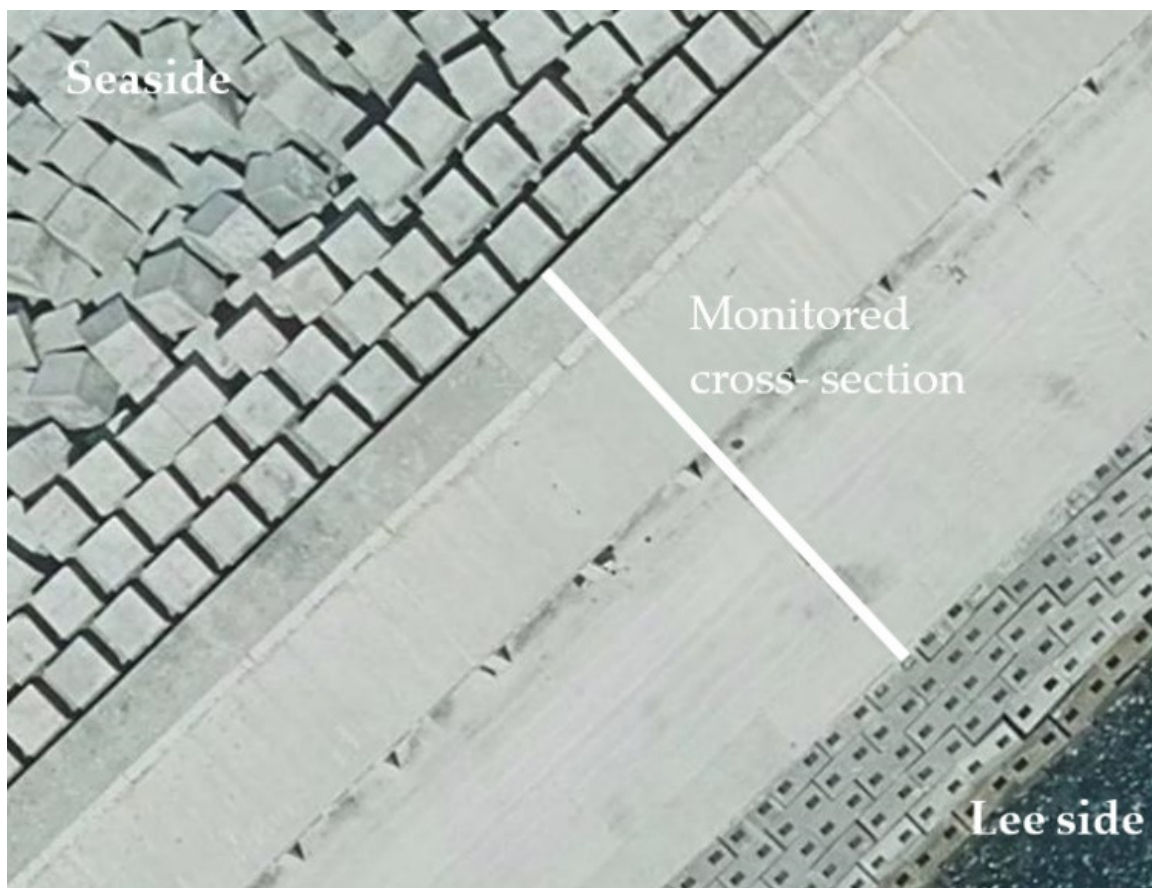


Figure 4. Aerial view of the monitored section.

3.2. Storm Events Analyzed

During the winters of 2017 and 2018, eight events occurred with measurements at pressure sensors. For these eight events, three-hourly values of significant wave height (H_s), maximum wave height (H_{max}), peak period (T_p), and wave directions (Dir) were also available. These wave characteristics were measured at a buoy located 2300 m from the breakwater, at a depth of 60 m. The tidal level was obtained using the tide gauge located on the spur breakwater and the range measure of this variable was from -0.5 m to $+4.57$ m in that location.

Table 2 summarizes the main characteristics of the wave and tidal level during the eight events. As can be seen in Table 2, H_s is higher than 7 m and H_{max} is higher than 9 m. Peak periods, T_p , vary from 14.3 s to large values of 20 s. The incident wave direction differs very little between the events, coming from the northwest and attacking the breakwater with an angle less than 20° . The sea level varies from almost high tide during storm events c and d , to almost low tide during storm events e to h .

Table 2. Wave and sea level characteristics during the eight storm events.

Storm Event	H_s (m)	H_{max} (m)	T_p (s)	Dir ($^\circ$ N)	Tidal Level (m)
<i>a</i>	10.78	14.80	19.20	329.00	2.66
<i>b</i>	9.69	13.81	20.00	327.00	3.16
<i>c</i>	10.65	14.86	18.90	327.00	3.40
<i>d</i>	10.78	13.98	19.70	327.00	3.33
<i>e</i>	8.45	12.49	15.40	334.00	1.46
<i>f</i>	7.21	10.58	14.30	332.00	1.41
<i>g</i>	7.09	9.87	14.30	330.00	1.94
<i>h</i>	9.40	14.10	20.00	319.00	1.06

3.3. Pressure Measured on the Crown Wall Front Wall

During the eight storm events presented in Table 2, time series of pressure at the pressure sensors with a frequency of 6 Hz were obtained. Figure 5 presents the time series of pressure measured (one hour in total) on the sensors during one of those storm events, storm h , and during the maximum pressure event registered.

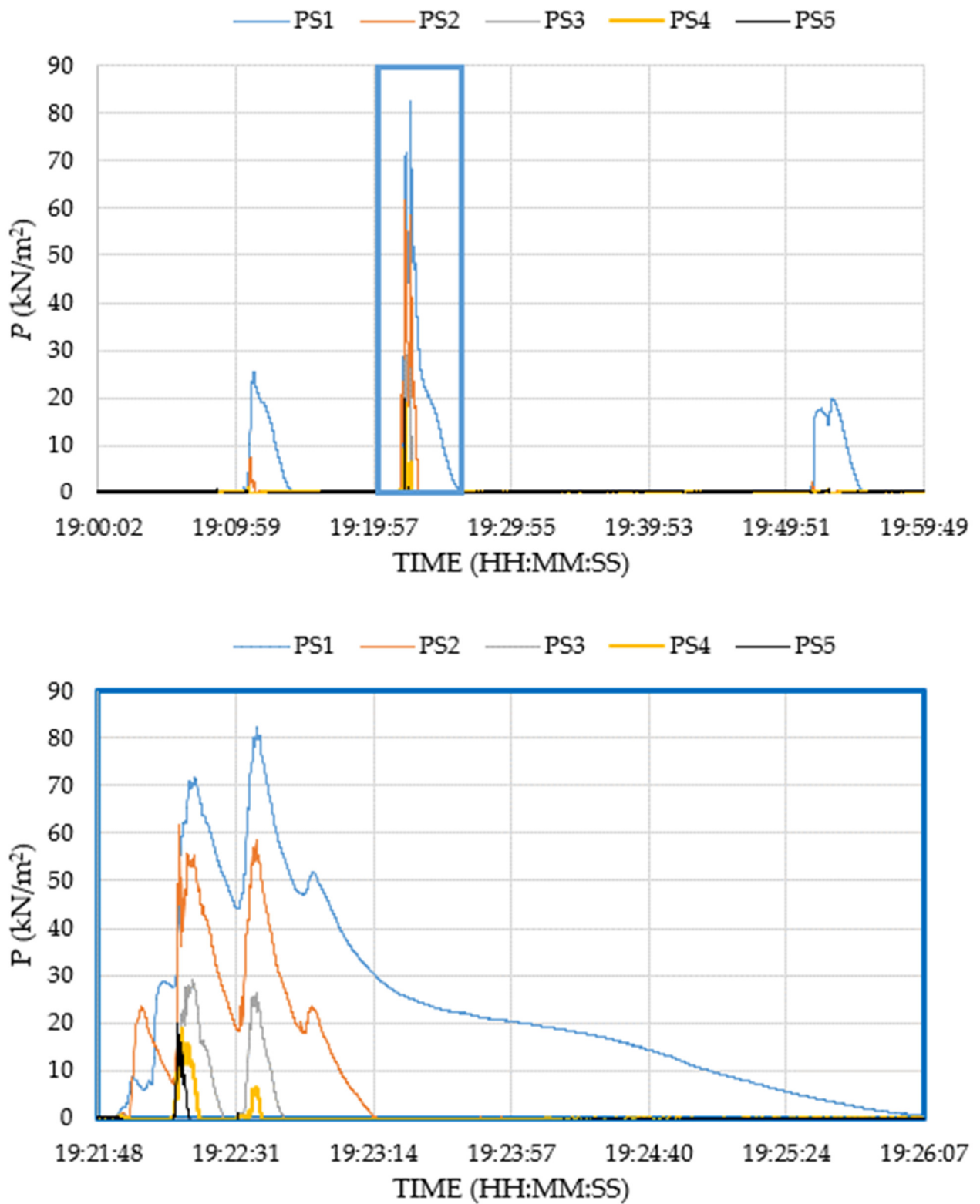


Figure 5. Time series of pressure measured at pressure sensors on 28 October 2017.

It can be seen how the pressure recorded by the sensors varies depending on their position, with two different behaviours being detected for different sensors: PS1 and PS2, located in the lower area of the crown wall; and PS3, PS4, and PS5 sensors, located in the higher part of the front wall of the structure. PS1 records the highest-pressure values and for a significantly longer duration than the other sensors. As can be seen in Figure 2, all sensors are always above the sea level. Therefore, the recorded pressure data are due to the runup after wave breaking over the outer armour layer of the breakwater or due to overtopping. In addition, this cross section has several peculiarities, as can be seen in Figure 2. One of them is the presence of a cube with its rubble mound foundation on the base of the crown wall, added during construction, and placed just in front of the pressure sensors PS1 and PS2, which acts as a barrier to the flow in this area, as referred to above. The water accumulated in that area causes large pressure values at PS1, which gradually decrease over the time, depending on the permeability of the core and filter layers. This accumulation of water registered in PS1 is also registered at PS2 sensor, located above the block core level, but with a smaller effect. PS3, PS4, and PS5 sensors have always registered lower pressures than at PS1 and PS2, being more related to water reaching the crown wall, from the armour layer or from the top of the structure owing to overtopping the crown wall.

To illustrate the results obtained, Table 3 presents the maximum pressure measured by each pressure sensor and the concomitant values of the rest of the sensors during the storm of 28 October 2017 in the 19:00 sea state (storm *h* in Table 2).

Table 3. Maximum pressure measured at the front face of the crown wall during the storm event that occurred on 28 October 2017 at the 19:00 sea state.

Time (hour:min:sec)	PS1 (kN/m ²)	PS2 (kN/m ²)	PS3 (kN/m ²)	PS4 (kN/m ²)	PS5 (kN/m ²)
19:22:12	35.38	39.89	12.67	7.49	19.80
19:22:14	58.87	36.04	20.98	18.86	15.75
19:22:17	70.40	53.75	29.00	10.71	-1.57
19:22:13	52.66	61.64	15.71	12.47	16.84
19:22:37	82.59	57.12	25.98	6.61	-1.76

As can be seen, each sensor reaches its own maximum pressure first at PS5 and at least at PS1. This seems to be caused by waves that overtopped the structure (and approach this section from the top to the bottom of the crown wall) crown wall and not by the impact of the wave impinging the structure. Moreover, as referred before, the crown wall is fully protected by the berm of the outer armour of the breakwater, so waves do not have direct impact to the crown wall. In fact, the same behaviour was found in all storm events analysed.

Table 4 summarizes the maximum pressure measured by the pressure sensors in each of the storm events divided by the *Hmax* obtained from the buoy; see Table 2.

Table 4. Maximum pressure measured at the sensors in each storm event.

Storm Event	<i>P/Hmax</i> (kN/m ³) at				
	PS1	PS2	PS3	PS4	PS5
<i>a</i>	1.28	0.20	0.12	0.04	0.14
<i>b</i>	2.12	0.11	0.06	0.04	0.40
<i>c</i>	1.13	0.15	0.12	0.09	0.29
<i>d</i>	4.09	2.50	0.58	0.08	0.10
<i>e</i>	2.17	0.28	0.06	0.04	0.10
<i>f</i>	0.20	0.05	0.05	0.07	0.15
<i>g</i>	0.72	0.08	0.04	0.05	0.10
<i>h</i>	5.86	4.37	2.06	1.34	1.40

As can be seen, in general, pressures are much higher in PS1 and PS2, as explained above. However, at PS3 to PS5, the pressures presented the same order of magnitude, all with values less than 0.58 kN/m³. The only exception is storm *h*, with the highest values of P/H_{max} obtained in all sensors. Storm *d* presents high values at SP1, reducing at PS2 and PS3 and having the same order of magnitude of the other storms at PS4 and PS5.

Figure 6 graphically shows the maximum pressures of each sensor in the eight storms analysed. Storms *a*, *b*, *c*, *d*, and *h* have, in general, the highest recorded P/H_{max} values. This is because they are the events with the most demanding wave conditions. However, at PS1, the storms with the highest H_{max} , storms *a* and *c*, present lower values than in other storms with lower values of H_{max} . The difference in results could also be because the measurements have been taken in just one cross section in a breakwater of more than 3000 m in length, where the maximum pressure values could occur in another zone, especially if it depends on overtopping. It is important to note that these eight storms analysed here have coincided with overtopping events on the instrumented section verified by no null pressure at the sensors placed at the crown of the gallery of the breakwater.

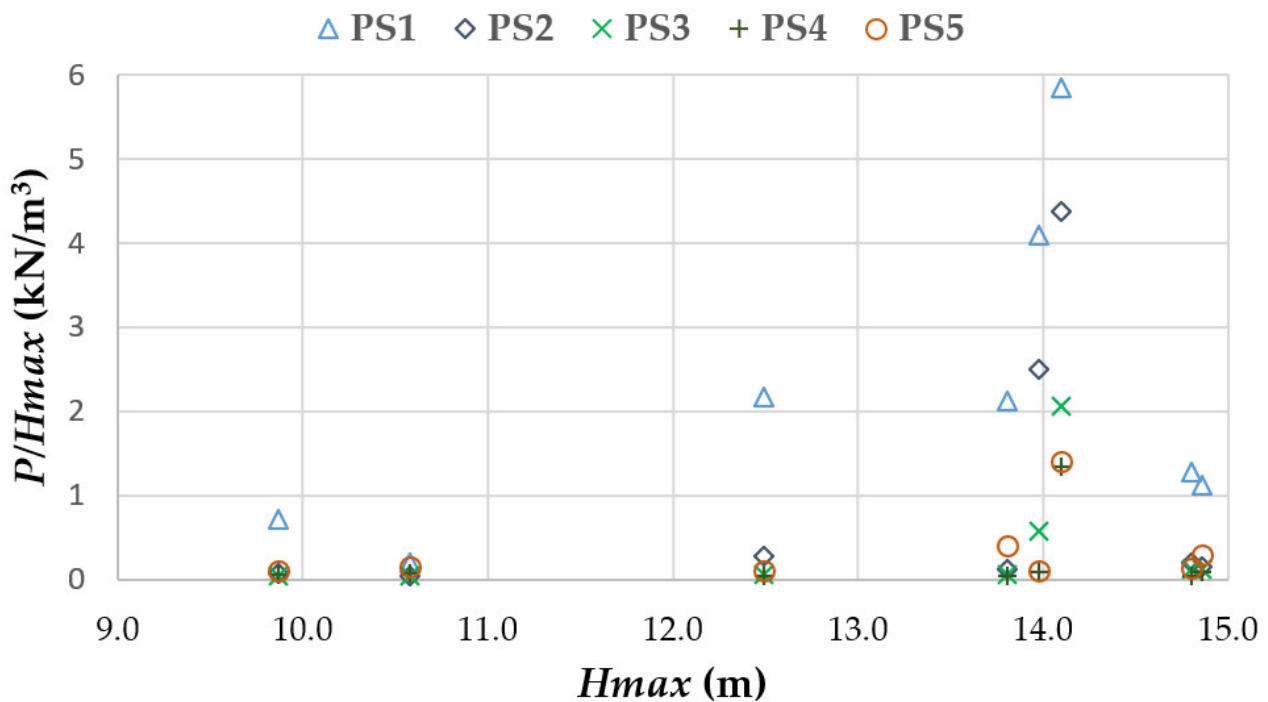


Figure 6. Maximum pressure measured on the storm events in each sensor.

Finally, in view of the analysis carried out on the measurements of the pressure sensors, as well as the conditioning factors owing to the section under analysis, it has been decided to select PS3, PS4, and PS5 sensors for the comparison of the maximum pressure measured with the resulting pressures estimated by state-of-the-art equations. In fact, the existing equations do not contemplate the effect of the placement of blocks that exist here in the core in front of the crown wall, which certainly affects the measurements on PS1 and PS2 sensors. As this structure has been found to have no influence on the measurements of the other three sensors, PS3 to PS5, the following study was proposed using only the three upper sensors.

4. Results

Pressure on the vertical face of the crown wall, calculated using formulas for the different storm events presented in Section 3.2, are presented here and compared with the pressure data obtained during the main field campaign at the main Punta Langosteira breakwater. Maximum pressures were obtained with formulas and compared with those measured for those pressure sensors selected on the vertical face of the crown wall during the field campaign.

4.1. Equation Application

The pressures on the superstructures of the rubble mound breakwaters fully protected by the armour layer are essentially due to the interaction between waves, filtered by the armour layer, and the superstructure, or due to overtopped waves reaching the superstructure.

4.2. Comparison of Pressure Data Measured and Estimated by Formulas

Günback and Gökçe (1984) [11] and Martín et al. (1999) [12] give null dynamic pressures for all storm events tested. In fact, run-up calculated by the formulas leads to non-overtopping conditions, contrary to that occurring in the field, where, for all storm events, overtopping had occurred. As the formula relates the different pressures with the run-up, R_u , and to the height of the armour berm, A_c , it leads to null dynamic pressure in the protected zone.

Martín et al. (1999) [12] is valid if the wave breaks before the superstructure of the bottom breaks ($\xi_{0p} > 3$), which occurs for all events tested when the range of $\xi_{0p,max}$ varies from 3.3 to 4.4. However, the data exceed the limits of expressions for calculating the λ parameter, representative of the decrease in dynamic pressure in the protected zone owing to the constituent materials of the main outer armour, because H/Lp is less than 0.03. So, the formula was applied outside its range of validity. Günback and Gökçe (1984) [11] do not impose validity limits on the equation. However, as referred to in Pereira et al. (2021) [21], the geometry considered in all of the formulas has the armour berm below the crest of the crown wall, and here, the crown wall is completely protected by the outer armour composed of cubes, which can lead to more overtopping conditions than with other blocks, which leads to larger wave dissipation.

Nørgaard et al.'s (2013) [15] formula was the only one that gives no null pressures for some of the storm events analysed here and, consequently, is the only one presented here. Sande et al. (2019) [27] used this formula to compare pressures measured with a physical model for this same port for the western breakwater (secondary breakwater), even with a slightly different cross section than the constructed one. They concluded that the formula represents the same behaviour of the wave forces on the crown wall, overestimating the pressures by not considering the effect of obliquity.

In 2013, Nørgaard, Lykke-Andersen, and Burcharth [15] proposed a modification to the formulation of Pedersen (1996) [13] with the aim of validating it for small depths, as it was originally limited to large and intermediate depths. The proposed modifications were based on the results of 162 tests on small-scale models and irregular wave action, considering agitation conditions at large and small depths and using the same experimental equipment used by Pedersen (1996) [13].

The first modification to the original formulation of Pedersen (1996) was made with respect to the runup only exceeded by 0.1% of the waves of the sea state considered, $R_{u,0.1\%}$ level. According to Nørsgaard et al. (2013) [15], the value of $R_{u,0.1\%}$ would now be given by the following:

$$R_{u,0.1\%} = \begin{cases} 0.603 H_{0.1\%} \xi_{0m} & \text{if } \xi_{0m} \leq 1.5 \\ 0.722 H_{0.1\%} \xi_{0m}^{0.55} & \text{if } \xi_m > 1.5 \end{cases} \quad (1)$$

where $H_{0.1\%}$ is the maximum wave height only exceeded by 0.1% of the waves of the sea states considered, given by Equation (2) according to Rayleigh’s distribution:

$$H_{0.1\%} = \frac{H_s}{0.538} \quad (2)$$

Knowing the value of $R_{u,0.1\%}$, and ignoring energy losses by friction, the ascending velocity of the water mass when run-up, v_0 , is given by the following:

$$v_0 = \sqrt{2g(R_{u,0.1\%} - A_c)} \quad (3)$$

The dynamic pressure in the protected area of the crown wall exceeded by only 0.1% of the waves of the sea states considered, $P_{d(p),0.1\%}$, is obtained by the following equation:

$$P_{d(p),0.1\%} = 0.5 \rho_w g \frac{v_0^2}{2g} = \rho_w g (R_{u,0.1\%} - A_c) \quad (4)$$

The formula is valid for $R_c/H_s < 2$, which occurs in three (storms *a*, *c*, and *d*) of the eight storm events analysed, although storm *b* has a close value, as shown in Figure 7.

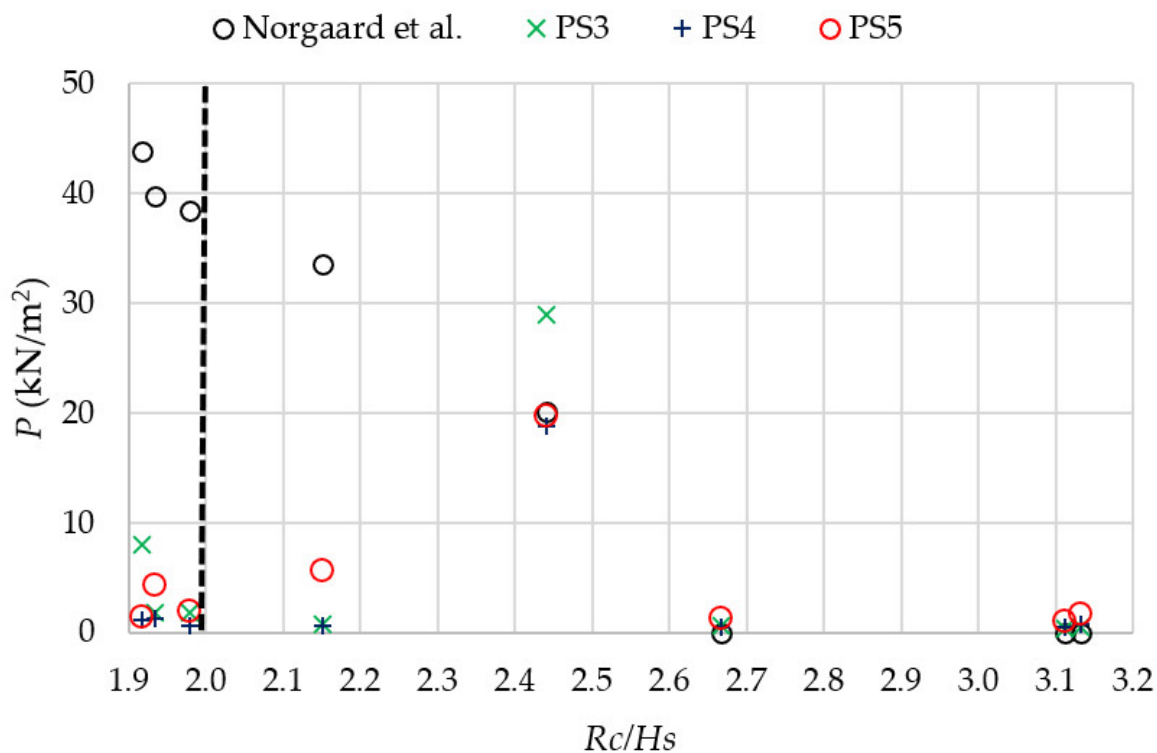


Figure 7. Horizontal pressure calculated by Nørsgaard et al. (2013) [15] and measured at sensors PS3 to PS5.

Table 5 summarizes the results obtained by the formula and compared with the maximum pressure obtained in pressure sensors PS3 to PS5, as the number of pressure events is very limited, meaning $P_{0.1\%}$ cannot be calculated.

Table 5. Maximum pressure calculated by Nørsgaard et al. (2013) [15] and measured in the sensors.

Storm Event	R_c/H_s (m)	$P_{Nørsgaard\ et\ al.}$ (kN/m ²)	Maximum Pressure (kN/m ²) at		
			PS3	PS4	PS5
<i>a</i>	1.98	38.51	1.83	0.59	1.99
<i>b</i>	2.15	33.53	0.78	0.57	5.58
<i>c</i>	1.93	39.80	1.82	1.26	4.31
<i>d</i>	1.92	43.88	8.06	1.18	1.44
<i>e</i>	2.67	0.00	0.69	0.49	1.24
<i>f</i>	3.13	0.00	0.48	0.69	1.62
<i>g</i>	3.11	0.00	0.40	0.48	0.97
<i>h</i>	2.44	20.08	29.00	18.85	19.80

Figure 7 presents the results obtained by the formula and the maximum pressure measured at pressure sensors PS3 to PS5 as a function of R_c/H_s .

The storm events presented different behaviours. For storms *a* to *d*, pressures estimated by the formula of Nørsgaard et al. (2013) [15] are much higher than those measured at PS3 to PS5. For storms *e* to *g*, Nørsgaard et al. (2013) [15], similar to Günback and Gökçe (1984) [11] and Martin et al. (1999) [12], give null pressures, contrary to the pressure sensors, which measured pressures up to 1.62 kN/m², with higher values being obtained at PS5. For storm *h*, the formula gives a maximum pressure similar to that measured at PS4 and PS5.

Storms *a* to *d* are almost within the application range of the formula for R_c/H_s , but as seen in Section 3.3, the maximum pressures occur first in PS5 and then in the lower ones, because the protection of the armour layer prevents the waves from directly impacting the sensor. Consequently, it seems that the registered pressures are mainly due to overtopping, leading to water penetrating between the blocks and the crown wall. This would explain why pressures are lower than those estimated by the equations and are higher in the pressure sensor located at a higher position and, in general, progressively reducing their values on the sensors located lower in the crown wall front face.

On the other hand, in storm events *e* to *g*, outside the validation limits of the equation, the pressures estimated by the formula are zero, corresponding to the low pressures recorded by the pressure sensors and to the less energetic weather conditions analysed for the breakwater under study.

The explanation that the authors have found for this different behaviour of the formula is the overtopping differences and three-dimensional effects due to the obliquity with which the waves arrive at the breakwater. To illustrate the referred effect of incident wave obliquity on the overtopping and measurements obtained from the sensors, Figure 8 shows overtopping events during storms *c* and *d*, both with high values of H_s and T_p and the same incident wave direction (see Table 2). In this figure, a red line has been marked at the monitored section. The image on the left shows the overtopping during storm event *c*, which occurs only at the monitored section. However, in storm *d*, overtopping occurs in several sections along the breakwater with different intensity. This explains why the pressure measured at only one monitored section could not reflect the overtopping that occurs over the levee. Consequently, it does not reflect either the pressure affected by overtopping at a crown wall or in a three-dimensional environment as in the field.



Figure 8. Aspect of overtopping event during (a) storm *c* and (b) storm *d* (monitoring section represented by a red line).

5. Conclusions

This study shows the field results of pressures on the crown wall front face fully protected by the armour layer. The existing equations were obtained through two-dimensional physical model tests, where the sensor is usually left directly exposed to the incidence of waves to measure the pressures on the crown wall. Moreover, when a crown wall of these characteristics is designed, it is assumed that pressure is constant along the whole structure. These facts become relevant when proposing crown wall designs with this type of breakwater typology.

The results obtained raise the importance of the correct location of the sensors in both laboratory and field campaigns. In laboratory tests, it is usual that different alignments of sensors are placed to analyse the pressure generated in the whole crown wall. However, it would be interesting to analyse the influence of their placement on crown walls protected by an armour layer with different porosities. Moreover, when planning field campaigns such as the current ones, it is important to locate the sensors in such a way that they allow the maximum possible information to be obtained.

An important aspect detected in the research is that, when the aerial view of the monitored section was analysed, it was noted that the sensors are placed behind a block of the armour layer. This is critical when an instrumentation is installed in a real section.

Moreover, this case study has peculiar characteristics that affect the measurements: there is a cubic block in front of the lowest level sensor position that generates a barrier to the flow, leading the accumulation of water in that area. This sensor is where the highest-pressure values were recorded and for a significantly longer duration than the other sensors. The accumulation of water registered in this sensor is not enough to significantly affect the measurement of the other sensors located above, located at the core level, and does not seem to affect other sensors, being more related to wave action crown wall. The maximum pressure occurs firstly in the sensor located at the highest level and is progressing to the bottom; it can be due to overtopping crown wall.

Pressures measured during eight storm events were compared to the state-of-the-art equations. In all storm events, pressures are no null and overtopping occurs. The equations of Günback and Gökçe (1984) [11] and Martin et al. (1999) [12] give null pressure results in all cases tested here. Nørgaard et al.'s (2013) [15] formulas were the only ones that give no null pressures, and thus were the ones used in this research. The cases with low pressures recorded by the pressure sensors and corresponding to less energetic weather conditions were outside the range of validity of the formulas. For those cases, the formula gives null pressures. For cases where higher pressures were measured, the formula of Nørgaard et al. (2013) [15] is valid and gives higher maximum pressures than the measured ones. This behaviour is possible because the crown wall is totally protected by the armour layer, and the pressure is measured at only one monitored section, not reflecting the overtopping that occurs over the whole breakwater. The results raise the importance of the correct location of the sensors in both the laboratory and field campaigns in such a way that they allow the maximum possible information to be obtained.

Author Contributions: Conceptualization, J.S., M.G.N., J.-S.L.-G., M.D.E., A.F., and V.N.; methodology, J.S., M.G.N., J.-S.L.-G., and M.D.E.; software, J.S. and M.G.N.; validation, J.S., M.G.N., J.-S.L.-G., M.D.E., A.F., and V.N.; formal analysis, J.S., M.G.N., J.-S.L.-G., M.D.E., A.F., and V.N.; investigation, J.S., M.G.N., J.-S.L.-G., M.D.E., A.F., and V.N.; writing—original draft preparation, J.S., M.G.N., J.-S.L.-G., and M.D.E.; writing—review and editing, J.S., M.G.N., J.-S.L.-G., M.D.E., A.F., and V.N.; supervision, J.S., M.G.N., J.-S.L.-G., M.D.E., A.F., and V.N. All authors have read and agreed to the published version of the manuscript.

Funding: Acknowledgement of the scientific and financial support by the Portuguese Foundation for Science and Technology (FCT) for project BSAFE4SEA—Breakwaters SAFETY control through a FORecast and decision support SystEm Analysis, Ref. PTDC/ECI-EGC/31090/2017.

Institutional Review Board Statement: Not applicable.

Informed Consent Statement: Not applicable.

Data Availability Statement: Data available upon request owing to privacy restrictions. The data are not publicly available for confidentiality reasons.

Acknowledgments: The authors are grateful to the Port Authority of A Coruña (Spain) and the Eptisa—Ingeniería, Instrumentación y Control (IIC) company for their kind collaboration and for sharing the information obtained in the Cormoran project. J.-S.L.-G. and M.D.E. are very grateful to LNEC for giving them the opportunity to perform research in the Hydraulics and Environment Department.

Conflicts of Interest: The authors declare no conflict of interest. The funders had no role in the design of the study; in the collection, analyses, or interpretation of data; in the writing of the manuscript; or in the decision to publish the results.

References

- Li, J.; Cheng, J.; Liu, S. An experimental study on the hydrodynamic performance of the twin vertical baffles underflow breakwater. *Ocean Eng.* **2022**, *256*, 111566. <https://doi.org/10.1016/j.oceaneng.2022.111566>.
- Mahmoudof, S.M.; Eyhavad-Koozhadi, A.; Bagheri, M. Field study of wave reflection from permeable rubble mound breakwater of Chabahar Port. *Appl. Ocean Res.* **2021**, *114*, 102786.
- Berenguer, J.M.; Baonza, A. On the design of crown walls of rubble mound breakwaters. In Proceedings of the 31st PIANC Congress, Estoril, Portugal, 14–18 May 2006; pp. 608–624.
- Lacasa, M.C.; Esteban, M.D.; López-Gutiérrez, J.S.; Negro, V.; Zang, Z. Feasibility study of the installation of wave energy converters in existing breakwaters in the north of Spain. *Appl. Sci.* **2019**, *9*, 5225.
- Han, X.; Jiang, Y.; Dong, S. Wave forces on crown wall of rubble mound breakwater under swell waves. *Ocean Eng.* **2022**, *259*, 111911. <https://doi.org/10.1016/j.oceaneng.2022.111911>.
- Negro, V.; Martín-Antón, M.; del Campo, J.M.; López-Gutiérrez, J.S.; Esteban, M.D. Crown walls in mass and reinforced concrete: The way to aesthetics in maritime works. In *Coasts, Marine Structures and Breakwaters 2017: Realising the Potential*; ICE Publishing, London, UK: 2018.
- Martín-Antón, M.; Negro, V.; del Campo, J.M.; López-Gutiérrez, J.S.; Esteban, M.D. The Impact of Public Works in Spain: Natural, constructed and destroyed landscape. *J. Constr.* **2017**, *16*, 82–91.
- Iribarren, R.; Nogales, C. *Obras Marítimas*. Dossat Ed. Madrid, Spain, 1964.
- Jensen, O.J. *A Monograph on Rubble Mound Breakwaters*; Danish Hydraulic Institute: Hørsholm, Denmark, 1984.
- Bradbury, A.P.; Allsop, N.W.H.; Stephens, R.V. *Hydraulic Performance of Breakwater Crown Walls*; Report SR146; HR Wallingford: Wallingford, UK, 1988.
- Günbak, A.R.; Gökçe, T. Wave screen stability of rubble-mound breakwaters. In Proceedings of the International Symposium of Maritime Structures in the Mediterranean Sea, Athens, Greece, 22–25 November 1984; pp. 2.99–2.112.
- Martín, F.L.; Losada, M.A.; Medina, R. Wave loads on rubble mound breakwater crown walls. *Coast. Eng.* **1999**, *37*, 149–174.
- Pedersen, J. Wave Forces and Overtopping on Crown Walls of Rubble Mound Breakwaters: An Experimental Study. PhD Thesis, Aalborg University, Aalborg, Denmark, 1996.
- Pedersen, J.; Burcharth, H.F. Wave force on crown walls. In Proceedings of the 23rd International Conference on Coastal Engineering, ASCE, Venice, Italy, 4–9 October 1992; pp. 1489–1502.
- Nørgaard, J.Q.H.; Andersen, T.L.; Burcharth, H.F. Wave loads on rubble mound breakwater crown walls in deep and shallow water wave conditions. *Coast. Eng.* **2013**, *80*, 137–147.
- Negro, V.; López-Gutiérrez, J.S.; Polvorinos Flors, J.I. Comparative study of breakwater crown wall—Calculation methods. *Proc. Inst. Civ. Eng. Marit. Eng.* **2013**, *166*, 25–41.
- Molines, J.; Herrera, M.P.; Medina, J.R. Estimation of wave forces on crown walls based on wave overtopping rates. *Coast. Eng.* **2018**, *132*, 50–62.

18. CIRIA/CUR/CETMEF. Physical processes and design tools: Crown walls. In *The Rock Manual: The Use of Rock in Hydraulic Engineering (2nd edition)*; CIRIA: London, United Kingdom, 2007.
19. United States Army Corps of Engineers (USACE). *Coastal Engineering Manual*; USACE: Washington, DC, USA, 2008.
20. Losada, M.A. Recent developments in the design of mound breakwaters. In *Handbook of Coast and Ocean Eng*; Gulf Publishing: Houston, TX, USA, 1990; pp. 939–1050.
21. Pereira, F.; Neves, M.G.; López-Gutiérrez, J.-S.; Esteban, M.D.; Negro, V. Comparison of Existing Equations for the Design of Crown Walls: Application to the Case Study of Ericeira Breakwater (Portugal). *J. Mar. Sci. Eng.* **2021**, *9*, 285. <https://doi.org/10.3390/jmse9030285>.
22. Webpage of Intergovernmental Panel on Climate Change (IPCC). Available online: www.ipcc.ch (accessed on 3 January 2021).
23. Diez, J.J.; Esteban, M.D.; Paz, R.; López-Gutiérrez, J.S.; Negro, V.; Monnot, J.V. Urban coastal flooding and climate change. *J. Coast. Res.* **2011**, *64*, 205–209.
24. Negro, V.; López-Gutiérrez, J.S.; Esteban, M.D.; del Campo, J.M.; Luengo, J. Action strategy for studying marine and coastal works with climate change on the horizon. *J. Coast. Res.* **2018**, *85*, 506–510.
25. Negro, V.; López-Gutiérrez, J.S.; Esteban, M.D.; Matutano, C. An analysis of recent changes in Spanish Coastal Law. *J. Coast. Res.* **2014**, *70*, 448–453.
26. Díaz-Sánchez, R.; López-Gutiérrez, J.S.; Lechuga, A.; Negro, V.; Esteban, M.D. Direct estimation wave setup as a medium level in swash. *J. Coast. Res.* **2013**, *65*, 201–206.
27. Sande, J.; Peña, E.; Maciñeira, E.; Figuero, A. 3D physical modelling for checking Level III probabilistic design in breakwaters: A case study in Punta Langosteira Port, Spain. *Coast. Eng. J.* **2019**, *61*, 460–471. <https://doi.org/10.1080/21664250.2019.1619987>.
28. Webpage of Port of A Coruña. Available online: <http://www.puertocoruna.com/es> (accessed on 29 July 2022).